

Chiral current in Floquet cavity-magnonics

Shi-fan Qi¹ and Jun Jing^{1,*}

¹*School of Physics, Zhejiang University, Hangzhou 310027, Zhejiang, China*

(Dated: June 22, 2022)

Floquet engineering could induce complex collective behaviour and interesting synthetic gauge-field in quantum many-body systems through temporal modulation of system parameters by periodic drives. Using a Floquet drive on frequencies of the magnon modes, we realize a chiral state-transfer in a hybrid photon-magnon system. The time-reversal symmetry is broken in such a promising platform for coherent information processing. The cavity-photon mode is adiabatically eliminated in the large-detuning regime and the magnon modes under conditional longitudinal drives can be indirectly coupled to each other with a phase-modulated interaction. The effective Hamiltonian is then used to generate chiral currents in a circular loop, whose dynamics is evaluated to measure the symmetry of the system Hamiltonian. Beyond the dynamics in the manifold with a limited number of excitations, our protocol applies to the continuous-variable systems with arbitrary initial states. In addition, it is found to be robust against the systematic errors in the photon-magnon coupling strength and Kerr nonlinearity.

I. INTRODUCTION

With unique properties such as large tunability, long coherent-time, and strong magnetic dipole-dipole interactions, the magnons can be used as the information carrier in a broad variety of hybrid systems [1–3]. Found to be strongly coupled to microwave photon [4–9], phonon [10–14], superconducting qubit [15–18], and spin-emitter [19, 20], they provide novel applications in quantum computing [21], quantum communication [22], and quantum sensing [23]. The “X-magnon” coupling motivates a number of foundational insights, e.g., the two-body flip-flop interaction of magnons for Rabi oscillation, which is symmetrical to time and parity. Nevertheless the complex-valued hopping between the magnons might support more flexible and interesting applications, such as generating chiral transfers of the quasiparticles of spin waves as a highly promising bosonic platform.

Chirality [24, 25] plays an important role in the fractional quantum Hall effect in the magnetic materials, that could be simulated by optical lattice [26]. Spin chirality arises from the three-body interactions, which has been experimentally realized in the platform of superconducting qubits [27]. The chirality operator of three spins is $\hat{O} = \vec{\sigma}_1 \cdot (\vec{\sigma}_2 \times \vec{\sigma}_3)$, where $\vec{\sigma}_j \equiv (\sigma_j^x, \sigma_j^y, \sigma_j^z)$ is the Pauli vector for the j th spin particle. It is straightforward to verify that \hat{O} breaks both the time reversal symmetry \mathcal{T} (replacing $\vec{\sigma}_j$ by $-\vec{\sigma}_j$) and the parity symmetry \mathcal{P} (exchanging $\vec{\sigma}_j$ with $\vec{\sigma}_k$) but conserves the \mathcal{PT} symmetry [27]. The dynamics of the spins driven by \hat{O} features a chiral evolution, i.e., $|s_1 s_2 s_3\rangle \rightarrow |s_2 s_3 s_1\rangle \rightarrow |s_3 s_1 s_2\rangle$, where $s_j = 0$ (spin down) or 1 (spin up) [28]. In parallel to the protocol in the superconducting qubits, we propose to generate a chiral transfer of an arbitrary bosonic state in the Floquet cavity-magnonic system [29]. Here

the system-Hamiltonian symmetry is described by a non-vanishing chiral current operator.

According to the Floquet theory [30–33], the propagator $U(t)$ induced by a time-dependent Hamiltonian $H(t) = H(t + T)$ with a period T can be expressed by $U(t) = U_F(t) \exp(-iH't)$, where $U_F(t)$ is also periodic with T and H' is a time-independent Hermitian operator. H' can be understood as the system Hamiltonian $H' = U_F^\dagger(t)H(t)U_F(t) - iU_F^\dagger(t)\dot{U}_F(t)$ in the periodically frame defined by $U_F(t)$. Floquet engineering by fast periodic modulation over the characteristic frequencies of a quantum system is a major control approach to the long-time dynamics of the system [31, 34–36], where the effective Hamiltonian can be synthesized through designing appropriate drives. Floquet engineering has been used to realize quantum switch [37], chiral ground state current [38], quantum simulation [39], and perfect state transfer [27, 40, 41] in superconducting qubits.

In this work, we apply the Floquet engineering to a hybrid photon-magnon system in which three single-crystal yttrium iron garnet (YIG) spheres are placed inside a microwave cavity. The uniform bias magnetic field excites the Kittel mode in the YIG spheres and establishes a strong photon-magnon coupling. At the large detuning regime, the common photon mode can be adiabatically eliminated with the standard perturbation theory [42–44] or the high-order Fermi golden rule [45]. By periodically modulating over the three magnon modes with well-controlled intensities, frequencies, and phases, we can obtain an effective time-reversal symmetry broken Hamiltonian [46], that ensures chiral magnon currents [38] of arbitrary states within a state-independent period. In contrast to the protocols based on the superconducting qubits [27, 38, 40], our protocol is not constrained in a manifold of a fixed number of excitations and is capable to transfer versatile states such as Fock state, coherent state, cat state, and even the two-body entangled states in a chiral way.

The rest part of this work is structured as follows. In Sec. II, we introduce the quantum model for a Flo-

* jingjun@zju.edu.cn

quet cavity-magnonic system and then derive an effective Hamiltonian to realize a perfect chiral state-transfer amongst magnons. The clockwise and anticlockwise transfers of various states and chiral currents to measure the symmetry of the system Hamiltonian are presented in Sec. III A and Sec. III B, respectively. We discuss the errors arise from the coupling strength of the photon-magnon interaction and the Kerr term in Sec. IV. And in Sec. V, we summarize the whole work.

II. MODEL

Consider a hybrid quantum model consists of a microwave cavity coupled to N YIG spheres in their Kittel modes [29]. The model Hamiltonian reads

$$H = \omega_a a^\dagger a + \omega_m \sum_{k=1}^N m_k^\dagger m_k + g_{am} \sum_{k=1}^N (a m_k^\dagger + a^\dagger m_k), \quad (1)$$

where a (a^\dagger) and m_k (m_k^\dagger) are the annihilation (creation) operators of the photon and the k th magnon modes, respectively. ω_a and ω_m are their respective transition frequencies. g_{am} is the single-excitation coupling strength between the photon and the magnon modes, which is much larger than the decay rates of both cavity mode and magnons and much smaller than $|\omega_a - \omega_m|$ in the dispersive (large detuning) regime.

When one focuses on the state-exchange within any pair of magnon modes, it is instructive to show that the photon mode could be adiabatically eliminated by the second-order perturbation theory [42]. The subsystem Hamiltonian associated with the k th and the j th magnon modes and the photon mode can be written as $H_0^{kj} + H_I^{kj}$, where

$$\begin{aligned} H_0^{kj} &= \omega_a a^\dagger a + \omega_m (m_k^\dagger m_k + m_j^\dagger m_j), \\ H_I^{kj} &= g_{am} [a (m_k^\dagger + m_j^\dagger) + a^\dagger (m_k + m_j)] \end{aligned} \quad (2)$$

indicating the unperturbed and perturbation Hamiltonians, respectively. To the second order in the perturbation Hamiltonian, the effective coupling strength g_{pq} between any pair of eigenstates $|p\rangle$ and $|q\rangle$ of H_0^{kj} in Eq. (2) is given by

$$g_{pq} = \sum_{w \neq p, q} \frac{\langle q | H_I^{kj} | w \rangle \langle w | H_I^{kj} | p \rangle}{E_p - E_w}, \quad (3)$$

where E_w is the eigenenergy of an intermediate eigenstate $|w\rangle$, namely, $H_0^{kj} |w\rangle = E_w |w\rangle$. Note that the large detuning condition $\omega_m \neq \omega_a$ lifts the degeneracy of H_0^{kj} . In the subspace with $n_k + n + n_j$ excitations, the leading contribution to Eq. (3) comes from two physical paths connecting $|n_k n n_j\rangle \equiv |n_k\rangle_k |n\rangle_a |n_j\rangle_j$ and $|(n_k - 1)n(n_j + 1)\rangle$, i.e., $|n_k n n_j\rangle \rightarrow |(n_k - 1)(n + 1)n_j\rangle \rightarrow |(n_k - 1)n(n_j + 1)\rangle$

and $|n_k n n_j\rangle \rightarrow |n_k(n - 1)(n_j + 1)\rangle \rightarrow |(n_k - 1)n(n_j + 1)\rangle$. Then we have

$$g_{n_k n_j} = \sqrt{n_k(n_j + 1)} \frac{g_{am}^2}{\omega_m - \omega_a}. \quad (4)$$

Note n_k , n , and n_j are arbitrarily nonnegative integers. The effective Hamiltonian for this pair of magnon modes in their full Hilbert space [12] can thus be written as

$$H_{kj} = g (m_k m_j^\dagger + m_k^\dagger m_j), \quad g \equiv \frac{g_{am}^2}{\omega_m - \omega_a}. \quad (5)$$

The preceding derivation as well as the formation of the effective Hamiltonian applies to any indirect magnon-magnon interaction mediated by the common photon mode. In the interaction picture, the Hamiltonian for the whole model in Eq. (1) can therefore be written as

$$H = g \sum_{k < j}^N (m_k m_j^\dagger + m_k^\dagger m_j). \quad (6)$$

We apply the periodic signals by Floquet driving featured with the intensity Δ , the frequency ω , and the local phases ϕ_k , to the model Hamiltonian and obtain

$$\begin{aligned} H(t) &= \Delta \sum_{k=1}^N \cos(\omega t + \phi_k) m_k^\dagger m_k \\ &+ g \sum_{k < j}^N (m_k m_j^\dagger + m_k^\dagger m_j). \end{aligned} \quad (7)$$

In the rotating frame with respect to

$$\begin{aligned} U_0(t) &= \exp \left[i \int_0^t ds \Delta \sum_{k=1}^N \cos(\omega s + \phi_k) m_k^\dagger m_k \right] \\ &= \exp \left\{ i \sum_{k=1}^N \frac{\Delta}{\omega} [\sin(\omega t + \phi_k) - \sin \phi_k] m_k^\dagger m_k \right\}, \end{aligned} \quad (8)$$

we have

$$\begin{aligned} H_I(t) &= U_0(t) H(t) U_0^\dagger(T) - i U_0(t) \dot{U}_0^\dagger(t) \\ &= \sum_{k < j}^N g_{kj} \exp [i f_{kj} \sin(\omega t + \alpha_{kj})] m_k^\dagger m_j + h.c., \end{aligned} \quad (9)$$

where

$$\begin{aligned} g_{kj} &= g e^{-i\beta_{kj}}, \quad \beta_{kj} \equiv \frac{\Delta}{\omega} (\sin \phi_k - \sin \phi_j), \\ f_{kj} &= \frac{2\Delta}{\omega} \sin \left(\frac{\phi_j - \phi_k}{2} \right), \\ \tan \alpha_{kj} &= \frac{\sin \phi_k - \sin \phi_j}{\cos \phi_k - \cos \phi_j}. \end{aligned}$$

According to the Jacobi-Anger expansion $e^{ix \sin y} = \sum_{n=-\infty}^{n=+\infty} J_n(x) e^{iny}$, where J_n is the n th Bessel function

of the first kind, one can obtain

$$H_I(t) = H_0 + \sum_{n=1}^{\infty} (H_n e^{in\omega t} + H_{-n} e^{-in\omega t}), \quad (10)$$

with

$$\begin{aligned} H_0 &= \sum_{k<j}^N J_0(f_{kj}) \left(g_{kj} m_k^\dagger m_j + g_{kj}^* m_k m_j^\dagger \right), \\ H_n &= \sum_{k<j}^N J_n(f_{kj}) e^{in\alpha_{kj}} \left[g_{kj} m_k^\dagger m_j + (-1)^n g_{kj}^* m_k m_j^\dagger \right], \end{aligned} \quad (11)$$

and $H_{-n} = H_n^*$. Therefore up to the order of $\mathcal{O}(1/\omega)$, the effective Floquet-driving Hamiltonian (7) can be written as

$$H_{\text{eff}} = H_0 + H_{\text{eff}}^{(2)} = H_0 + \sum_{n=1}^{\infty} \frac{1}{n\omega} [H_n, H_{-n}]. \quad (12)$$

Under the Floquet driving, we have several remarkable observations. (a) The zeroth-order coupling-strength between the k th and the j th magnon is $g_{kj} J_0(f_{kj})$, which can be tuned by the ratio of the driving intensity and frequency Δ/ω and the phase difference between the local driving signals $\phi_k - \phi_j$. (b) When $N = 2$, the leading-order correction by the commutator $[H_n, H_{-n}]$ vanishes and then the dynamics of magnons is a Rabi oscillation with a frequency fully determined by f_{kj} . (c) When $N > 2$, the leading-order correction can be written as

$$H_{\text{eff}}^{(2)} = \sum_{k<j} \left(g_{kj}^{(2)} e^{i\alpha_{kj}} m_k^\dagger m_j + h.c. \right), \quad (13)$$

where the second-order coupling strength is

$$g_{kj}^{(2)} \sim \frac{g^2}{\omega} \sum_{k_1 \neq k, j} \left[\sum_{n=1}^{\infty} \frac{J_n(f_{kk_1}) J_n(f_{k_1 j})}{n} \right], \quad (14)$$

with k_1 indicating the other magnon modes except k and j in the whole system.

The third and even higher orders of terms can be analyzed with the James' effective-Hamiltonian method [34]. The nonvanishing third-order terms in the effective Hamiltonian can be obtained by

$$\begin{aligned} H_{kj}^{(3)} &= \sum_{l=m+n} \frac{1}{(n+m)\omega^2} [H_n, [H_m, H_{-l}]] \\ &= \sum_{k<j} \left(g_{kj}^{(3)} e^{i\alpha_{kj}} m_k^\dagger m_j + h.c. \right), \end{aligned} \quad (15)$$

where the third-order coupling strength $g_{kj}^{(3)}$ is about

$$\sim \frac{g^3}{\omega^2} \sum_{k_1 \neq k, k_2 \neq j} \left[\sum_{l=m+n} \frac{J_n(f_{kk_1}) J_m(f_{k_1 k_2}) J_l(f_{k_2 j})}{n+m} \right]. \quad (16)$$

Therefore the third and even higher orders of corrections can be safely omitted in the dispersive regime $g \ll \omega$.

Chiral state-transfer (as described in Fig. 1) could manifest when $N = 3$ by setting $\phi_j = 2\pi j/3$, $j = 1, 2, 3$, which are uniformly distributed in the range of $[0, 2\pi]$. In this case, the magnitude of the ratio factor f_{kj} becomes independent of the magnon pair, i.e., $f_{12} = f_{13} = f_{23} = \sqrt{3}\Delta/\omega \equiv f$. Otherwise it is hard to observe a perfect chiral current. The relevant quantum phases are found to be $\beta_{12} = f$, $\beta_{23} = -f/2$, $\beta_{13} = f/2$; and $\alpha_{12} = \pi/2$, $\alpha_{13} = 5\pi/6$, $\alpha_{23} = 7\pi/6$, i.e., $\alpha_{kj} = (k+j)\pi/3 - \pi/2$. Then using H_n in Eq. (11), the second-order term in the effective Hamiltonian (12) turns out to be

$$H_{\text{eff}}^{(2)} = -ig_{\text{eff}} \sum_{j=k+1} \left(e^{-i\beta_{kj}} m_k^\dagger m_j - e^{i\beta_{kj}} m_k m_j^\dagger \right). \quad (17)$$

Note if $k = 3$, then $j = 1$, and

$$g_{\text{eff}} = g_{\text{eff}}(f) = \frac{2g^2}{\omega} \sum_{n=1}^{\infty} \frac{J_n^2(f)}{n} \sin\left(\frac{n\pi}{3}\right). \quad (18)$$

Consequently, the effective Hamiltonian in Eq. (12) can be expressed by an coefficient matrix,

$$H_{\text{eff}} = [m_1^\dagger, m_2^\dagger, m_3^\dagger] \begin{bmatrix} 0 & G^* e^{-if} & G e^{-if/2} \\ G e^{if} & 0 & G^* e^{if/2} \\ G^* e^{if/2} & G e^{-if/2} & 0 \end{bmatrix} \begin{bmatrix} m_1 \\ m_2 \\ m_3 \end{bmatrix}, \quad (19)$$

where $G = gJ_0(f) + ig_{\text{eff}}$ is the effective coupling strength. Using $\tan \phi \equiv g_{\text{eff}}/[gJ_0(f)]$, the Hamiltonian has a more compact form,

$$H_{\text{eff}} = |G| [m_1^\dagger, m_2^\dagger, m_3^\dagger] \begin{bmatrix} 0 & e^{i\phi_{12}} & e^{-i\phi_{31}} \\ e^{-i\phi_{12}} & 0 & e^{i\phi_{23}} \\ e^{i\phi_{31}} & e^{-i\phi_{23}} & 0 \end{bmatrix} \begin{bmatrix} m_1 \\ m_2 \\ m_3 \end{bmatrix}, \quad (20)$$

where $\phi_{12} = -\phi - f$, $\phi_{23} = -\phi + f/2$, and $\phi_{31} = -\phi + f/2$. The eigenvalues of the coefficient matrix satisfies $E^3 - 3E - 2 \cos \Phi = 0$, where $\Phi \equiv \phi_{12} + \phi_{23} + \phi_{31} = -3\phi$ is defined as the closed-loop phase up to $2n\pi$ with n an integer. The system dynamics is then found to be solely determined by the driving intensity and frequency rather than the ratio factor f . Φ is thus regarded as the synthetic magnetic flux. It is gauge-invariant by noting that in our model the three YIGs form a closed loop and the accumulated phase of the state-current (either chiral or not) has to be single-valued when going around this loop. $\Phi = 0$ or π corresponds to the absence of the Floquet engineering. Then the evolution of the magnons is symmetrical when one of the magnons (say mode-1) is prepared at the target state and the rest two are in the same states. The quantum state propagates from mode-1 to mode-2 and mode-3 simultaneously and then back to mode-1. This pattern repeats itself with no indication of any preferred circulation direction.

III. NUMERICAL SIMULATION OF CHIRAL CURRENTS

A. Chiral state transfer

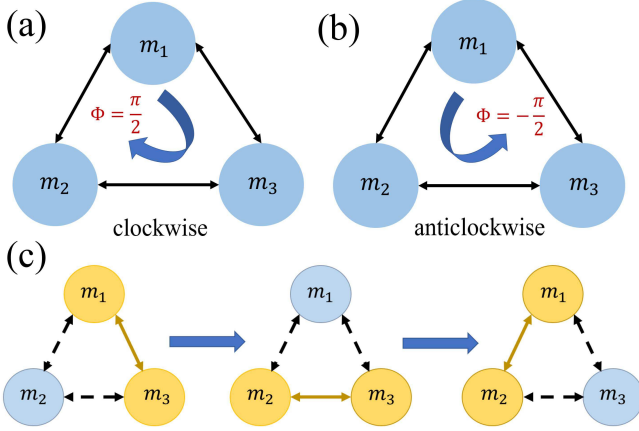


FIG. 1. (a) and (b): The diagrams of the chiral state transfers in the magnons along the clockwise and the anticlockwise directions, respectively. (c): The diagram of the chiral entanglement transfer along the clockwise direction, where two yellow circles connected by a solid line represent the two entangled magnons and the blue circle describes a separable magnon.

With a Hamiltonian similar to Eq. (20), which was obtained by the tunneling-term modulation [38] rather than the longitudinal Floquet driving, it was demonstrated that the time-reversal symmetry can be broken when the loop phase $\Phi = \pm\pi/2$. This idea can be generalized to realize a chiral state-transfer in our continuous-variable system for arbitrary target states.

Due to Eq. (19), $\Phi = \pi/2$ means $G = ig_{\text{eff}}$ under the condition of $J_0(f) = 0$ (Note it is not appropriate for $N \geq 4$, in which all of f_{kj} 's cannot be the same in magnitude). It renders that $f = \sqrt{3}\Delta/\omega = 2.4048$ [Consequently $J_1(f) = 0.5192$, $J_2(f) = 0.4318$, $J_3(f) = 0.1990$, $J_4(f) = 0.0647$, $J_5(f) = 0.0164$, $J_6(f) = 0.0034$, et.al.]. Thus the Hamiltonian becomes

$$H_{\text{eff}} = ig_{\text{eff}} [m_1^\dagger, m_2^\dagger, m_3^\dagger] \begin{bmatrix} 0 & -e^{-if} & e^{-if/2} \\ e^{if} & 0 & -e^{if/2} \\ -e^{if/2} & e^{-if/2} & 0 \end{bmatrix} \begin{bmatrix} m_1 \\ m_2 \\ m_3 \end{bmatrix}. \quad (21)$$

The canonical transformation in the Heisenberg picture then can be written as

$$\begin{bmatrix} m_1(t) \\ m_2(t) \\ m_3(t) \end{bmatrix} = T(t) \begin{bmatrix} m_1(0) \\ m_2(0) \\ m_3(0) \end{bmatrix} \quad (22)$$

with

$$T(t) = \frac{1}{3} \begin{bmatrix} x(t) & e^{-if}y(t) & e^{-\frac{if}{2}}z(t) \\ e^{if}z(t) & x(t) & e^{\frac{if}{2}}y(t) \\ e^{\frac{if}{2}}y(t) & e^{-\frac{if}{2}}z(t) & x(t) \end{bmatrix}, \quad (23)$$

where

$$\begin{aligned} x(t) &= 1 + 2 \cos(\sqrt{3}g_{\text{eff}}t), \\ y(t) &= 1 - 2 \cos(\sqrt{3}g_{\text{eff}}t + \frac{\pi}{3}), \\ z(t) &= 1 - 2 \cos(\sqrt{3}g_{\text{eff}}t - \frac{\pi}{3}). \end{aligned} \quad (24)$$

With respect to the time-evolved operator, it is interesting to find that $m_3(t) = m_1(0)$ and $m_2(t) = m_3(0)$ when $t = (2\pi/3 + 2n\pi)/(\sqrt{3}g_{\text{eff}})$; $m_2(t) = m_1(0)$ and $m_3(t) = m_2(0)$ when $t = (4\pi/3 + 2n\pi)/(\sqrt{3}g_{\text{eff}})$; and $m_j(t) = m_j(0)$ when $t = 2n\pi/(\sqrt{3}g_{\text{eff}})$ with n an integer. This transfer is exactly described by the clockwise rotation $m_1 \rightarrow m_3 \rightarrow m_2 \rightarrow m_1$ in Fig. 1(a), corresponding to a chiral evolution in the Schrödinger picture, i.e., $|\varphi_1\varphi_2\varphi_3\rangle \rightarrow |\varphi_2\varphi_3\varphi_1\rangle \rightarrow |\varphi_3\varphi_1\varphi_2\rangle$, where φ_j is arbitrary for the j th mode.

In addition, during the operator-transformation process of $m_1 \rightarrow m_3$, the matrix element $|z(t)|$ that measures the occupation probability of the mode m_2 is found to be maximized in magnitude when $t = (\pi/3 + 2n\pi)/(\sqrt{3}g_{\text{eff}})$. It means at those moments, we have the maximal population over the second mode, which is undesired for $m_1 \rightarrow m_3$. Similarly, when $t = (5\pi/3 + 2n\pi)/(\sqrt{3}g_{\text{eff}})$, the occupation probability of m_3 is expected to achieve the maximum value during $m_1 \rightarrow m_2$.

The state-transfer fidelity in the Schrödinger picture can be measured by the time-dependent state population $P_j(t)$, $j = 1, 2, 3$, for the j th magnon mode. To avoid the influence from the local dynamical phases [14], it can be defined by

$$P_j(t) = \sum_{C_n \neq 0} |\langle \varphi(t) | n \rangle_j|^2. \quad (25)$$

Here the initial state of the full system is supposed to be $|\varphi(0)\rangle = \sum_n C_n |n00\rangle \equiv \sum_n C_n |n\rangle_1 |0\rangle_2 |0\rangle_3$ with the normalized coefficients C_n , i.e., the first magnon is prepared as an arbitrary target state and the other two are in their ground states. The dynamics of the magnons is analytically determined by Eq. (22) or numerically calculated by the Floquet-driving Hamiltonian in Eq. (7).

For $|\varphi(0)\rangle = |100\rangle$, we have

$$|\varphi(t)\rangle = \frac{1}{3} \left[x(t)|100\rangle + e^{-if}z(t)|010\rangle + e^{-\frac{if}{2}}y(t)|001\rangle \right]. \quad (26)$$

While for an arbitrary superposed state

$$|\varphi(0)\rangle = \sum_n C_n |n00\rangle = \sum_n \frac{C_n}{\sqrt{n!}} \left[m_1^\dagger(0) \right]^n |000\rangle, \quad (27)$$

the time-evolved state can be written as

$$|\varphi(t)\rangle = \sum_n \frac{C_n}{\sqrt{n!}} \left[\sum_j m_j^\dagger(0) T_{j1}^\dagger(t) \right]^n |000\rangle. \quad (28)$$

Then due to Eqs. (22) and (23), we have $\varphi(t_3) = \sum_n C_n |00n\rangle$ at the desired time $t_3 = 2\pi/(3\sqrt{3}g_{\text{eff}})$ and

$\varphi(t_2) = \sum_n C_n |0n0\rangle$ at $t_2 = 4\pi/(3\sqrt{3}g_{\text{eff}})$, up to certain local phases. Based on Eq. (28), one can even transfer a mixed state by $\rho(t) = \sum_j p_j |\varphi(t)\rangle_{jj} \langle\varphi(t)|$.

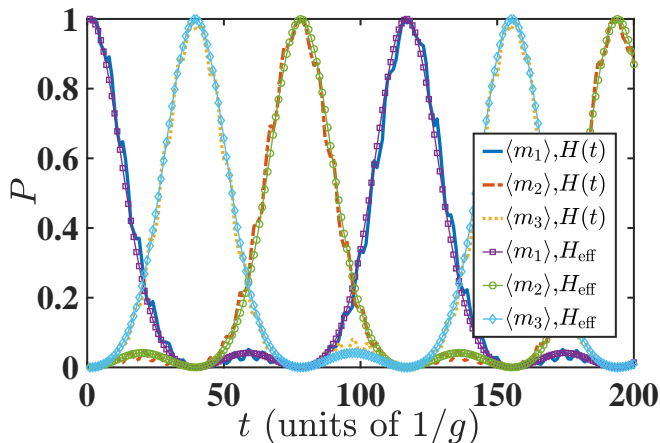


FIG. 2. Time evolutions of the state populations $P_j(t)$, $j = 1, 2, 3$, for the three magnons by the numerical simulation with the Floquet-driving Hamiltonian (7) and the analytical evaluation with the canonical transformation (22). The initial state is $|\varphi(0)\rangle = 1/\sqrt{3} \sum_{n=1}^3 |n00\rangle$. The other parameters are set $\omega = 20g$ and $\phi_j = 2\pi j/3$.

Figure 2 is used to verify the time evolutions of the state populations $P_j(t)$ by the effective Hamiltonian (21) as well as the canonical transformation (22) in comparison with that by the Floquet-driving Hamiltonian (7) under the condition of $J_0(f) = 0$. It is found the analytical results (lines with markers) do match with their numerical counterparts (lines without markers) for the normalized evolution times. And the transfer period is irrespective to the chosen initial state.

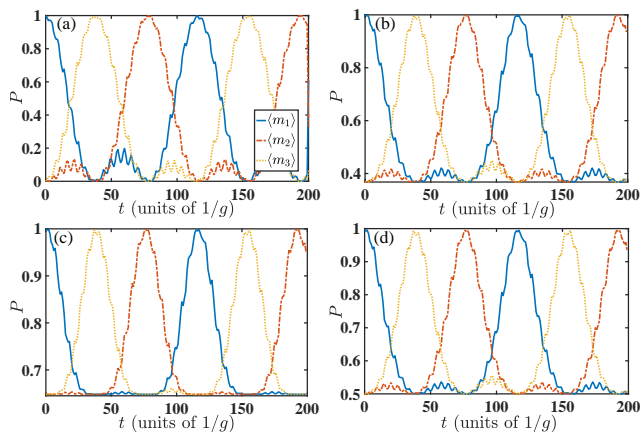


FIG. 3. The clockwise state-transfer of the three magnons described by their state populations under the Floquet-driving Hamiltonian (7). The initial states of the magnon-mode m_1 are (a) the Fock state $|n = 1\rangle$, (b) the coherent state with $\beta = 1$, (c) the cat state with $\zeta = 1$, and (d) the thermal state with $\bar{n} = 1$. The other parameters are set $\omega = 20g$ and $\phi_j = 2\pi j/3$.

In Fig. 3, it is interesting to show that the chiral transfer protocol is applicable to the Fock state, the coherent state, the cat state $(|\zeta\rangle + |-\zeta\rangle)/\sqrt{2 + 2e^{-2|\zeta|^2}}$ with $|\zeta\rangle$ the Glauber coherent state, and the Gibbs thermal state $\rho = \sum_n p_n |n\rangle\langle n|$ with the Fock-state occupation $p_n = (\bar{n})^n / (1 + \bar{n})^{n+1}$ and the average excitation number \bar{n} . The maximal value for all the state populations during the clockwise state-transfer approaches to unit indicating a perfect transfer amongst m_1 , m_2 , and m_3 . Figures. 2 and 3 demonstrate that the Floquet-driving Hamiltonian in Eq. (21) under the condition $J_0(f)$ would ensure a high-fidelity chiral state-transfer for arbitrary target states.

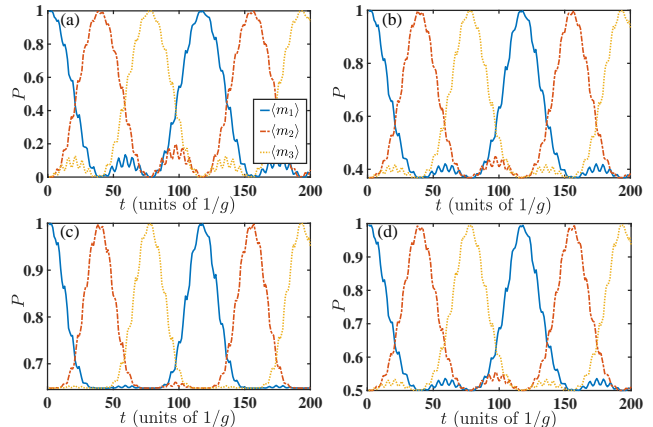


FIG. 4. The anticlockwise state-transfer of the three magnons described by their state populations under the Floquet-driving Hamiltonian (7). The initial states of the magnon-mode m_1 are (a) the Fock state $|n = 1\rangle$, (b) the coherent state with $\beta = 1$, (c) the cat state with $\zeta = 1$, and (d) the thermal state with $\bar{n} = 1$. Here the parameters are set $\omega = 20g$, $\phi_1 = 2\pi/3$, $\phi_2 = 2\pi$, and $\phi_3 = 4\pi/3$.

By setting $\phi_1 = 2\pi/3$, $\phi_2 = 2\pi$, and $\phi_3 = 4\pi/3$, which is an alternative uniform distribution of ϕ_j in the range of $[0, 2\pi]$, the coefficient matrix in Eq. (19) becomes

$$\begin{bmatrix} 0 & Ge^{-if/2} & G^*e^{-if} \\ G^*e^{if/2} & 0 & G^*e^{if/2} \\ Ge^{if} & Ge^{if/2} & 0 \end{bmatrix} \quad (29)$$

where $G = gJ_0(f) - ig_{\text{eff}}$. That induces the synthetic magnetic flux with $\Phi = -\pi/2$. It amounts to exchange the magnon mode-2 and 3, that gives rise to the anticlockwise circulation as shown in Fig 1(b). Then the effective Hamiltonian in Eq. (21) is modified to

$$H_{\text{eff}} = ig_{\text{eff}} [m_1^\dagger, m_2^\dagger, m_3^\dagger] \begin{bmatrix} 0 & e^{-if/2} & -e^{-if} \\ -e^{if/2} & 0 & -e^{-if/2} \\ e^{if} & e^{if/2} & 0 \end{bmatrix} \begin{bmatrix} m_1 \\ m_2 \\ m_3 \end{bmatrix}. \quad (30)$$

Through a canonical transformation similar to Eq. (22), one can easily achieve the anticlockwise state-transfer. For example, the time-dependent state $|\varphi(t)\rangle$ in Eq. (26)

for the single-excitation state becomes

$$|\varphi(t)\rangle = \frac{1}{3} \left[x(t)|100\rangle + e^{-\frac{if}{2}}y(t)|010\rangle + e^{-if}z(t)|001\rangle \right], \quad (31)$$

where $x(t)$, $y(t)$, and $z(t)$ are given by Eq. (24). The numerical results for Fock state, coherent state, cat state, and thermal state are shown in Fig. 4, exhibiting the opposite chirality. During the anticlockwise state-transfer $m_1 \rightarrow m_2 \rightarrow m_3$, all the magnon modes achieve a nearly unit fidelity in a periodical sequence. It demonstrates that the anticlockwise chiral state-transfer could be also realized for all states.

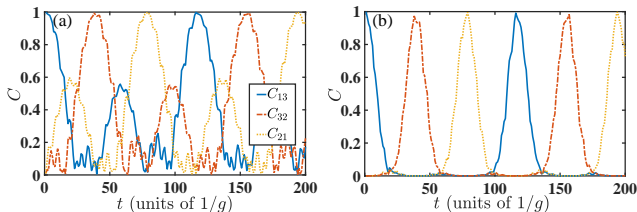


FIG. 5. The clockwise transfer of the pairwise concurrence in the three-magnon system under the Floquet-driving Hamiltonian (7). Initially, the magnon mode-1 and mode-3 are set as (a) the Bell state $(|00\rangle + |11\rangle)/\sqrt{2}$ and (b) the NOON state $(|0N\rangle + |N0\rangle)/\sqrt{2}$ with $N = 5$. The other parameters are the same as Fig. 2.

If two magnons in our model could be prepared as an entangled state and the third one is separably initialized at the ground state, we can demonstrate a high-fidelity chiral transfer for the pairwise quantum entanglement [see Fig. 1(c)]. In particular, we consider that mode-1 and mode-3 are prepared as the double-excitation Bell state $(|00\rangle + |11\rangle)/\sqrt{2}$ or the NOON state $(|0N\rangle + |N0\rangle)/\sqrt{2}$ under the clockwise-transfer condition, i.e., $\Phi = \pi/2$.

It is well known that the concurrence could be used as a sufficient and necessary entanglement criterion for any pure-state bipartite system and any two-state bipartite system. According to its definition [47] for a two-qubit system AB , $C = \max\{0, \lambda_1 - \lambda_2 - \lambda_3 - \lambda_4\}$, where λ_j are the square root of the eigenvalues of $\rho_{AB}(\sigma_y^A \otimes \sigma_y^B)\rho_{AB}^*(\sigma_y^A \otimes \sigma_y^B)$ in the decreasing order. For a pure state $a|11\rangle + b|10\rangle + c|01\rangle + d|00\rangle$ with normalized coefficients, its concurrence can be easily derived as $C = 2|bc - ad|$.

Inspired by the expression for the pure state, we here employ a modified concurrence to measure the chiral-transfer of the entangled state in our model. If the initial state is the Bell state $(|00\rangle + |11\rangle)/\sqrt{2}$, then the concurrence between mode- j and mode- k is defined as $C_{jk} = |\langle\varphi(t)|00\rangle_{jk}| |\langle\varphi(t)|11\rangle_{jk}|$; and if the initial state is chosen as the NOON state $(|0N\rangle + |N0\rangle)/\sqrt{2}$, then $C_{jk} = |\langle\varphi(t)|0N\rangle_{jk}| |\langle\varphi(t)|N0\rangle_{jk}|$. These definitions amount to the original occurrence when the perfect state-transfer is realized and become sufficient but not necessary for the states during the time evolution, which is calculated with the Floquet-driving Hamiltonian (7).

In Fig. 5, the blue solid lines, the red dot-dashed lines, and the yellow dotted lines represent the concurrence between mode-1 and mode-3, between mode-3 and mode-2, and between mode-2 and mode-1, respectively. It is found that both the Bell state and the NOON state could be faithfully transferred in a chiral way along the magnon triangle. At the desired moments due to Eq. (24), one can observe a nearly maximally-entangled state. The result is independent of the choice of N . Our model then widens the application range of the chiral state-transfer.

B. Chiral current

The appearance of the ground-state chiral edge-current is a key signature of fractional quantum Hall states. And the chiral current is an effective measure for the symmetry of the system Hamiltonian in condensed matter systems. Using the current operator defined in Ref. [38], we now consider the continuity equation for each magnon mode, e.g., $\partial_t \hat{n}_k = I_{\text{in}} - I_{\text{out}}$, where $\hat{n}_k \equiv m_k^\dagger m_k$ is the occupation operator of the k th magnon mode and I_{in} (I_{out}) represents the input (output) current with respect to mode- k . Under the necessary condition of the clockwise transfer in Fig. 1(a), $\phi_j = 2\pi j/3$, $j = 1, 2, 3$, we have three equations of motion:

$$\begin{aligned} \partial_t \hat{n}_1 &= I_{12} - I_{31} = i[H_{\text{eff}}, \hat{n}_1], \\ \partial_t \hat{n}_2 &= I_{23} - I_{12} = i[H_{\text{eff}}, \hat{n}_2], \\ \partial_t \hat{n}_3 &= I_{31} - I_{23} = i[H_{\text{eff}}, \hat{n}_3], \end{aligned} \quad (32)$$

where H_{eff} is the effective Hamiltonian in Eq. (19) or Eq. (20) and I_{jk} represents the current from mode- j to mode- k . Then we have

$$\begin{aligned} I_{12} &= iG e^{if} m_1 m_2^\dagger - iG^* e^{-if} m_1^\dagger m_2, \\ I_{31} &= -iG^* e^{-if/2} m_1 m_3^\dagger + iG e^{if/2} m_1^\dagger m_3, \\ I_{23} &= iG e^{-if/2} m_2 m_3^\dagger - iG^* e^{if/2} m_2^\dagger m_3. \end{aligned} \quad (33)$$

Normalized by the coupling-strength $|G|$ of H_{eff} , the effective current operator from mode- j to mode- k can be defined as

$$\hat{I}_{kj} = i e^{-i\phi_{kj}} m_k m_j^\dagger - i e^{i\phi_{kj}} m_k^\dagger m_j. \quad (34)$$

Accordingly, the circle current operator is defined as $\hat{I} = \hat{I}_{12} + \hat{I}_{23} + \hat{I}_{31}$. It is straightforward to find that the circle current operator is an integral of motion due to that it commutes with the system Hamiltonian, i.e., $[H_{\text{eff}}, \hat{I}] = 0$. It means that the expectation value of $\langle \hat{I} \rangle$ can not be used to measure the time-reversal symmetry of our model.

We have known that the magnon system has a symmetrical evolution for a synthetic magnetic flux $\Phi = 0$ or $\Phi = \pi$ under the effective Hamiltonian in Eq. (20). In case that mode-1 is initialized as an arbitrary target state, the state or excitations will propagate to mode-2 and mode-3 simultaneously and periodically go back to

mode-1. Consequently, the current $\langle \hat{I}_{23} \rangle$ from mode-2 to mode-3 vanishes. A nonzero current $\langle \hat{I}_{23} \rangle$ appears when $\Phi \neq 0, \pi$ and becomes maximum when the time-reversal symmetry is broken, i.e., $\Phi = \pm\pi/2$. We check the condition $\Phi = \pi/2$ under $\phi_j = 2\pi j/3$. Using $|\varphi(t)\rangle$ in Eq. (26) with the initial Fock state $|100\rangle$, it is found that

$$\langle \hat{I}_{23}(t) \rangle = \frac{4}{9} \left[2 \cos^2(\sqrt{3}g_{\text{eff}}t) - \cos(\sqrt{3}g_{\text{eff}}t) - 1 \right]. \quad (35)$$

It attains the maximal value $\langle \hat{I}_{23}^{\text{max}} \rangle = 8/9$ when $\sqrt{3}g_{\text{eff}}t = \pi + 2n\pi$. Given an arbitrary state in Eq. (28), we have

$$\langle \hat{I}_{23}^{\text{max}} \rangle = \frac{8}{9} \sum_n n C_n^2 = \frac{8}{9} \bar{n}, \quad (36)$$

where \bar{n} is the average excitation number of the target state. For a coherent state $|\beta\rangle$, $\bar{n} = |\beta|^2$ and for a cat state $(|\zeta\rangle + |-\zeta\rangle)/\sqrt{2 + 2e^{-2|\zeta|^2}}$, $\bar{n} = |\zeta|^2[1 - \exp(-2|\zeta|^2)]/[1 + \exp(-2|\zeta|^2)]$. Then the expectation value of $\langle \hat{I}_{23}(t) \rangle$ is effective to measure the time-reversal or parity-reversal symmetry of the system Hamiltonian.

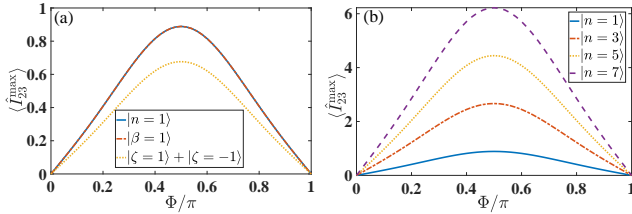


FIG. 6. (a) The maximal value of the current from m_2 to m_3 as the function of the closed-loop phase Φ under the effective Hamiltonian (20). The initial states are the Fock state $|n=1\rangle$ (the blue solid line), the coherent state with $\beta=1$ (the red dot-dashed line), and the cat state with $\zeta=1$ (the yellow dotted line). (b) The maximal value of the current from m_2 to m_3 for various Fock states.

The preceding analysis is consistent with the numerical simulation in Fig. 6, where we plot $\langle \hat{I}_{23}^{\text{max}} \rangle$ with the close-loop phase or the synthetic magnetic field Φ . It is found that the maximal current vanishes when $\Phi = 0$ and $\Phi = \pi$. It can be understood that at these points, the system Hamiltonian becomes real that cannot break the time-reversal symmetry. Otherwise, any finite Φ breaks the symmetry and leads to the chiral currents. It is interesting to find in Fig. 6(a) that the maximal currents for the Fock state $|n=1\rangle$ and the coherent state with $\beta=1$ are equivalent to each other. Both of them are equal to $0.89 \approx 8/9$ at the peak point $\Phi = \pi/2$. They are larger than the cat state with $\zeta=1$, whose peak value at $\Phi = \pi/2$ is 0.68. Thus a larger average excitation number yields a larger $\langle \hat{I}_{23}^{\text{max}} \rangle$ with the same Φ . This result can also be supported by Fig. 6(b), in which a monotonic pattern appears with increasing n .

IV. FIDELITY UNDER SYSTEMATIC ERRORS

Our model in Eq. (1) has been discussed under the ideal condition that all the coupling strengths g_{am} between photon and magnon modes are the same in magnitude. While in practice [2, 7], they are associated with the individual locations of the YIG spheres in the cavity. We first consider the systematic errors raised by the nonequal coupling strengths. In particular, we suppose that $g_{am}^{(1)} = g_{am}$, $g_{am}^{(2)} = g_{am}(1 + \delta)$, and $g_{am}^{(3)} = g_{am}(1 - \delta)$, where the superscript $j \in \{1, 2, 3\}$ marks the coupling strength between the common photon and the j th magnon and δ is used to estimate the magnitude of the relative error. With $N=3$, the system Hamiltonian in Eq. (1) is then rewritten as

$$\begin{aligned} H = & \omega_a a^\dagger a + \omega_m \sum_{k=1}^3 m_k^\dagger m_k + g_{am} (am_1^\dagger + a^\dagger m_1) \\ & + g_{am}(1 + \delta) (am_2^\dagger + a^\dagger m_2) \\ & + g_{am}(1 - \delta) (am_3^\dagger + a^\dagger m_3). \end{aligned} \quad (37)$$

Under the conditions that $\phi_j = 2\pi j/3$ and $J_0(f) = 0$ for the clockwise chiral transfer, the effective Hamiltonian in Eq. (21) is modified by changing the coefficient matrix to be

$$ig_{\text{eff}} \begin{bmatrix} 0 & -(1 - \delta^2)e^{if} & (1 + \delta)e^{if/2} \\ (1 - \delta^2)e^{-if} & 0 & -(1 - \delta)e^{-if/2} \\ -(1 + \delta)e^{-if/2} & (1 - \delta)e^{if/2} & 0 \end{bmatrix}. \quad (38)$$

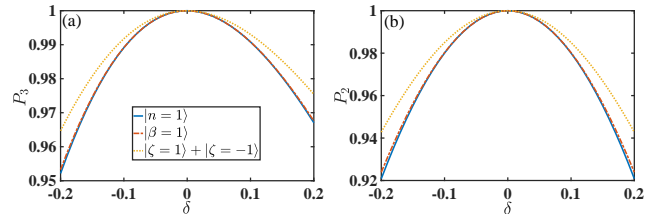


FIG. 7. (a) The state population of the 3rd magnon at the desired moment $t_3 = 2\pi/(3\sqrt{3}g_{\text{eff}})$ and (b) The state population of the 2nd magnon at the desired moment $t_2 = 4\pi/(3\sqrt{3}g_{\text{eff}})$ as a function of the magnitude of the relative error δ under the effective Hamiltonian (38). The initial states are the Fock state $|n=1\rangle$ (the blue solid line), the coherent state with $\beta=1$ (the red dot-dashed line), and the cat state with $\zeta=1$ (the yellow dotted line).

In Fig. 7, we present the sensitivity of the state populations [see Eq. (25)] to the systematic error δ at the desired moments for the chiral state-transfer obtained by Eq. (24). It is found that the robustness of our model against the systematic errors becomes weaker with a larger average population. The cat state with $\zeta=1$ is found to be more robust in comparison with the Fock state $|n=1\rangle$ and the coherent state with $\beta=1$. For all of them, both transferred populations of mode-2 and

mode-3 could be maintained above 0.98 in the presence of about 10% errors or fluctuations in the photon-magnon coupling strength.

Another systematic error in our model is associated with the nonlinearity in the expansion of the YIG crystal or the dipolar anisotropy energy quadratic in the magnon numbers, which is parameterized with the Kerr coefficient K . When the excitation number in the spin wave is much smaller than the total number of spins in YIG sphere, the system Hamiltonian in Eq. (6) can be modified to [8, 48]

$$\tilde{H}_{\text{Kerr}} = g \sum_{k < j}^N \left(m_k m_j^\dagger + m_k^\dagger m_j \right) + \sum_k K \left(m_k^\dagger m_k \right)^2. \quad (39)$$

For a YIG sphere with a typical size about 250 μm , the Kerr coefficient $K/2\pi \approx 6.4 \times 10^{-9}$ Hz, which is much smaller than the effective coupling strength g . The coupling strength between photon and magnon is found to be $g_{\text{am}}/2\pi \approx 20$ MHz in recent experiments [6, 15, 16], which means that the effective coupling strength g in Eq. (5) could be about 1 MHz in magnitude. Given the timescale we considered in the preceding chiral dynamics, we can safely apply our model in such a hybrid photon-magnon system when the number of the excited spins $\langle m_k^\dagger m_k \rangle$ are less than 10^6 .

V. CONCLUSION

In summary, we have proposed a chiral state-transfer proposal in a Floquet cavity magnon system, which consists of a microwave cavity coupled to three YIG spheres in their Kittler modes. The three magnon modes constitute a triangle loop of mutual interaction by eliminating the photon mode in a state-resolved way. The longitudinal driving with proper parameters forms complex coupling strengths of magnons, that generates a tunable synthetic magnetic flux. Our results open a path towards simulation of a time-reversal-broken many-body continuous-variable system that can realize the chiral transfer for arbitrary states. It is beyond the limitation of fixed excitation numbers in literature. We also evaluate the chiral current to measure the symmetry of the system Hamiltonian. The stability of our proposal is tested with its sensitivity to the systematic errors in the coupling strength and the nonlinear terms in the system. Our work in pursuit of the quantum chiral state transfer provides an important application in cavity magnonics as a promising hybrid platform for control over the emerging phases.

ACKNOWLEDGMENTS

We acknowledge financial support from the National Science Foundation of China (Grants No. 11974311 and No. U1801661).

-
- [1] B. Z. Rameshti, S. V. Kusminskiy, J. A. Haigh, K. Usami, D. Lachance-Quirion, Y. Nakamura, C.-M. Hu, H. X. Tang, G. E. Bauer, and Y. M. Blanter, *Cavity magnonics*, arxiv: 2106.09312v1 (2021).
- [2] D. Lachance-Quirion, Y. Tabuchi, A. Gloppe, K. Usami, and Y. Nakamura, *Hybrid quantum systems based on magnonics*, *Appl. Phys. Express* **12**, 070101 (2019).
- [3] Y. Li, W. Zhang, V. Tyberkevych, W. K. Kwok, and V. Novosad, *Hybrid magnonics: physics, circuits, and applications for coherent information processing*, *J. Appl. Phys.* **128**, 130902 (2020).
- [4] O. O. Soykal and M. E. Flatté, *Strong field interactions between a nanomagnet and a photonic cavity*, *Phys. Rev. Lett.* **104**, 077202 (2010).
- [5] O. O. Soykal and M. E. Flatté, *Size dependence of strong coupling between nanomagnets and photonic cavities*, *Phys. Rev. B* **82**, 104413 (2010).
- [6] Y. Tabuchi, S. Ishino, T. Ishikawa, R. Yamazaki, K. Usami, and Y. Nakamura, *Hybridizing ferromagnetic magnons and microwave photons in the quantum limit*, *Phys. Rev. Lett.* **113**, 083603 (2014).
- [7] X. Zhang, C.-L. Zou, L. Jiang, and H. X. Tang, *Strongly coupled magnons and cavity microwave photons*, *Phys. Rev. Lett.* **113**, 156401 (2014).
- [8] Y.-P. Wang, G.-Q. Zhang, D. Zhang, T.-F. Li, C.-M. Hu, and J. Q. You, *Bistability of cavity magnon polaritons*, *Phys. Rev. Lett.* **120**, 057202 (2018).
- [9] R.-C. Shen, Y.-P. Wang, J. Li, S.-Y. Zhu, G. S. Agarwal, and J. Q. You, *Long-time memory and ternary logic gate using a multistable cavity magnonic system*, *Phys. Rev. Lett.* **127**, 183202 (2021).
- [10] X. Zhang, C.-L. Zou, L. Jiang, and H. Tang, *Cavity magnonmechanics*, *Sci. Adv.* **2**, e1501286 (2016).
- [11] J. Li, S.-Y. Zhu, and G. S. Agarwal, *Magnon-photon-phonon entanglement in cavity magnomechanics*, *Phys. Rev. Lett.* **121**, 203601 (2018).
- [12] S.-f. Qi and J. Jing, *Magnon-assisted photon-phonon conversion in the presence of structured environments*, *Phys. Rev. A* **103**, 043704 (2021).
- [13] J. Li, Y.-P. Wang, W.-J. Wu, S.-Y. Zhu, and J. You, *Quantum network with magnonic and mechanical nodes*, *PRX Quantum* **2**, 040344 (2021).
- [14] S.-f. Qi and J. Jing, *Accelerated adiabatic passage in cavity magnomechanics*, *Phys. Rev. A* **105**, 053710 (2022).
- [15] D. Lachance-Quirion, S. Piotr Wolski, Y. Tabuchi, S. Kono, K. Usami, and Y. Nakamura, *Entanglement-based single-shot detection of a single magnon with a superconducting qubit*, *Science* **367**, 425 (2020).
- [16] Y. Tabuchi, S. Ishino, A. Noguchi, T. Ishikawa, R. Yamazaki, K. Usami, and Y. Nakamura, *Coherent coupling between a ferromagnetic magnon and a superconducting qubit*, *Science* **349**, 405 (2015).

- [17] S.-f. Qi and J. Jing, *Generation of bell and greenberger-horne-zeilinger states from a hybrid qubit-photon-magnon system*, *Phys. Rev. A* **105**, 022624 (2022).
- [18] J.-s. Yan and J. Jing, *External-level assisted cooling by measurement*, *Phys. Rev. A* **104**, 063105 (2021).
- [19] T. c. v. Neuman, D. S. Wang, and P. Narang, *Nanomagnonic cavities for strong spin-magnon coupling and magnon-mediated spin-spin interactions*, *Phys. Rev. Lett.* **125**, 247702 (2020).
- [20] S.-f. Qi and J. Jing, *Magnon-mediated quantum battery under systematic errors*, *Phys. Rev. A* **104**, 032606 (2021).
- [21] T. D. Ladd, F. Jelezko, R. Laflamme, Y. Nakamura, C. Monroe, and J. L. O'Brien, *Quantum computers*, *Nature (London)* **464**, 45 (2010).
- [22] A. Reiserer and G. Rempe, *Cavity-based quantum networks with single atoms and optical photons*, *Rev. Mod. Phys.* **87**, 1379 (2015).
- [23] C. L. Degen, F. Reinhard, and P. Cappellaro, *Quantum sensing*, *Rev. Mod. Phys.* **89**, 035002 (2017).
- [24] P. Lodahl, S. Mahmoodian, S. Stobbe, A. Rauschenbeutel, P. Schneeweiss, J. Volz, H. Pichler, and P. Zoller, *Chiral quantum optics*, *Nature* **541**, 473 (2017).
- [25] H. Zhu, J. Yi, M.-Y. Li, J. Xiao, L. Zhang, C.-W. Yang, R. A. Kaindl, L.-J. Li, Y. Wang, and X. Zhang, *Observation of chiral phonons*, *Science* **359**, 579 (2018).
- [26] A. S. Sørensen, E. Demler, and M. D. Lukin, *Fractional quantum hall states of atoms in optical lattices*, *Phys. Rev. Lett.* **94**, 086803 (2005).
- [27] W. Liu, W. Feng, W. Ren, D.-W. Wang, and H. Wang, *Synthesizing three-body interaction of spin chirality with superconducting qubits*, *Appl. Phys. Lett.* **116**, 114001 (2020).
- [28] H. Cai and D.-W. Wang, *Topological phases of quantized light*, *Nat. Sci. Rev.* **8**, nwaa196 (2021).
- [29] J. Xu, C. Zhong, X. Han, D. Jin, L. Jiang, and X. Zhang, *Floquet cavity electromagnonics*, *Phys. Rev. Lett.* **125**, 237201 (2020).
- [30] J. H. Shirley, *Solution of the schrödinger equation with a hamiltonian periodic in time*, *Phys. Rev.* **138**, B979 (1965).
- [31] N. Goldman and J. Dalibard, *Periodically driven quantum systems: Effective hamiltonians and engineered gauge fields*, *Phys. Rev. X* **4**, 031027 (2014).
- [32] M. Bukov, L. D'Alessio, and A. Polkovnikov, *Universal high-frequency behavior of periodically driven system: from dynamical stabilization to floquet engineering*, *Adv. in Phys.* **64**, 139 (2015).
- [33] F. Petiziol, M. Sameti, S. Carretta, S. Wimberger, and F. Mintert, *Quantum simulation of three-body interactions in weakly driven quantum systems*, *Phys. Rev. Lett.* **126**, 250504 (2021).
- [34] W. Shao, C. Wu, and X.-L. Feng, *Generalized james' effective hamiltonian method*, *Phys. Rev. A* **95**, 032124 (2017).
- [35] D.-W. Wang, H. Cai, R.-B. Liu, and M. O. Scully, *Mesoscopic superposition states generated by synthetic spin-orbit interaction in fock-state lattices*, *Phys. Rev. Lett.* **116**, 220502 (2016).
- [36] H. Li, H. Cai, J. Xu, V. V. Yakovlev, Y. Yang, and D.-W. Wang, *Quantum photonic transistor controlled by an atom in a floquet cavity-qed system*, *Opt. Express* **27**, 6946 (2019).
- [37] Y. Wu, L.-P. Yang, M. Gong, Y. Zheng, H. Deng, Z. Yan, Y. Zhao, K. Huang, A. D. Castellano, W. J. Munro, K. Nemoto, D.-N. Zheng, C. Sun, Y.-x. Liu, X. Zhu, and L. Lu, *An efficient and compact switch for quantum circuits*, *npj. Quantum Inf.* **4**, 50 (2018).
- [38] P. Roushan, C. Neill, A. Megrant, Y. Chen, R. Babbush, R. Barends, B. Campbell, Z. Chen, B. Chiaro, A. Dunsworth, A. Fowler, E. Jeffrey, J. Kelly, E. Lucero, J. Mutus, P. ÓMalley, M. Neeley, C. Quintana, D. Sank, A. Vainsencher, J. Wenner, T. White, E. Kapit, H. Neven, and J. Martinis, *Chiral ground-state currents of interacting photons in a synthetic magnetic field*, *Nat. Phys.* **13**, 146 (2017).
- [39] O. Kyriienko and A. S. Sørensen, *Floquet quantum simulation with superconducting qubits*, *Phys. Rev. Applied* **9**, 064029 (2018).
- [40] D.-W. Wang, C. Song, W. Feng, and et al., *Synthesis of antisymmetric spin exchange interaction and chiral spin clusters in superconducting circuits*, *Nat. Phys.* **15**, 382 (2019).
- [41] X. Li, Y. Ma, J. Han, T. Chen, Y. Xu, W. Cai, H. Wang, Y. Song, Z.-Y. Xue, Z.-q. Yin, and L. Sun, *Perfect quantum state transfer in a superconducting qubit chain with parametrically tunable couplings*, *Phys. Rev. Applied* **10**, 054009 (2018).
- [42] L. Garziano, V. Macrì, R. Stassi, O. Di Stefano, F. Nori, and S. Savasta, *One photon can simultaneously excite two or more atoms*, *Phys. Rev. Lett.* **117**, 043601 (2016).
- [43] K. K. W. Ma and C. K. Law, *Three-photon resonance and adiabatic passage in the large-detuning rabi model*, *Phys. Rev. A* **92**, 023842 (2015).
- [44] B. Kaufman, T. Rozgonyi, P. Marquetand, and T. Weinacht, *Adiabatic elimination in strong-field light-matter coupling*, *Phys. Rev. A* **102**, 063117 (2020).
- [45] M. Combescot, *On the generalized golden rule for transition probabilities*, *J. Phys. A: Math. Gen.* **34**, 6087 (2001).
- [46] J. Koch, A. A. Houck, K. L. Hur, and S. M. Girvin, *Time-reversal-symmetry breaking in circuit-qed-based photon lattices*, *Phys. Rev. A* **82**, 043811 (2010).
- [47] W. K. Wootters, *Entanglement of formation of an arbitrary state of two qubits*, *Phys. Rev. Lett.* **80**, 2245 (1998).
- [48] Y.-P. Wang, G.-Q. Zhang, D. Zhang, X.-Q. Luo, W. Xiong, S.-P. Wang, T.-F. Li, C.-M. Hu, and J. Q. You, *Magnon kerr effect in a strongly coupled cavity-magnon system*, *Phys. Rev. B* **94**, 224410 (2016).